Inelastic electron-electron scattering in silicon (100) inversion layers

K. K. Choi
Yale University, Section of Applied Physics, P.O. Box 2157, New Haven, Connecticut 06520-2159
(Received 24 February 1983; revised manuscript received 16 May 1983)

In a weakly disordered system where $kT\tau_e/\hbar \sim 1$, we find experimentally that the electron inelastic scattering rate deduced from the magnetoconductance measurement is separable into a T^2 term and a T term, which agree with the theoretical calculations on the electron-electron interaction in the ordered and diffusive limits. Since the scattering process formulated in the diffusive limit is momentum nonconserving, it affects conductivity directly. This idea is supported by the data published earlier by Cham and Wheeler.

I. INTRODUCTION

Among the different electron scattering mechanisms in solids, electron-electron scattering has played an unimportant role in the transport properties in most materials. Recently, electron-electron scattering has been invoked as the principal mechanism to delocalize electrons in order to explain the magnetoconductance measurements in silicon inversion layers. The magnetoconductance effect in such a system provides a probe for the first time to investigate the characteristics of electron-electron interaction.

From the magnetoconductance measurements, the inelastic scattering time (τ_i) can be extracted. While the magnitude τ_i is consistent among different experimental groups, the explicit temperature dependences observed are slightly different depending upon the experimental conditions. In order to clarify this issue, more precise measurements are desirable.

II. ELECTRON-ELECTRON SCATTERING

Electron-electron scattering has been known to be affected by the amount of impurities or dislocations in the medium. The effect of the impurities on the scattering was investigated by Schmid.[1] He found that the rate of such scattering is enhanced by the presence of impurities in bulk metals. In addition to the normal T^2-dependent term, there is an extra $T^{3/2}$ term that depends on the disorder of the system. The scattering rate in three dimensions can be expressed as

$$\frac{1}{\tau_i}=\frac{\pi}{8}\frac{(kT)^2}{\hbar E_F}+\frac{\sqrt{3}}{2}\left[\frac{\hbar}{2E_F\tau_e}\right]^{3/2}\frac{(kT)^{3/2}}{\hbar E_F^{1/2}}\ , \tag{1}$$

where τ_e is the electron-impurity scattering time. The contribution from the second term increases as the electron-impurity scattering time or Fermi energy decreases. On the other hand, when there are no impurities, only the first term exists. Schmid attributed the second term to the momentum-nonconserving processes, which result from the loss of the translational invariance introduced by the defects in an impure conductor.

Recently, electron-electron interaction has been reexamined in the two-dimensional (2D) case.[2-4] In the ordered limit ($E_F\tau_e/\hbar \gg kT\tau_e/\hbar \gg 1$) the inelastic scattering time (τ_i) is found to be

$$\frac{1}{\tau_i}=\frac{\pi}{2}\frac{(kT)^2}{\hbar E_F}\ln\frac{E_F}{kT}\ . \tag{2}$$

Whereas in the diffusive case ($E_F\tau_e/\hbar \gg 1 \gg kT\tau_e/\hbar$), τ_i is given by

$$\frac{1}{\tau_i}=\frac{kT}{2E_F\tau_e}\ln\frac{T_1}{T}\ , \tag{3}$$

where $kT_1=\hbar^3D^3\kappa^4/e^4$ in cgs units, $D=\frac{1}{2}V_F^2\tau_e$, $\kappa=2\pi Ne^2$.

Equation (3) is the contribution from the momentum-nonconserving processes. This can be seen from the formalism that the density-density correlation function is of the diffusion type.[3] Furthermore, this term vanishes in the absence of impurities. So, in general, when $kT\tau_e/\hbar \sim 1$, both terms from Eqs. (2) and (3) should contribute. Usually, in metallic systems, $k_Fl \sim 2E_F\tau_e/\hbar$ is very large, due to the large Fermi energy, so that the second term in Eq. (1) is negligible in comparison with the momentum-conserving term. For instance, for potassium at around 1 K, k_Fl is approximately equal to 8×10^5 with resistivity around 2.4×10^{-13} Ω m. So for normal undoped metals, the second term in Eq. (1) is less than the leading term by 6 orders of magnitude. However, in silicon inversion layers, the situation is very different from a metal due to the small Fermi energy. From the device parameters used in this paper, $\tau_e=7.4\times10^{-13}$ s at $E_F=2\times10^{-21}$ J, $N_s=2\times10^{16}$ m^{-2}, and $k_Fl=28$. This makes the magnitude of $1/\tau_i$ given by Eqs. (2) and (3) comparable. For instance, at $N_s=2\times10^{16}$ m^{-2}, $1/\tau_i$ given by Eq. (2) is $6.1\times10^9T^2$ s^{-1}, and $1/\tau_i$ given by Eq. (3) is $1.2\times10^{11}T$ s^{-1}. So at low T the momentum-nonconserving term can be dominant.

This argument is consistent with the experimental observation[5-9] that $1/\tau_i \sim T^p$, where p is within the range 1–2 at the temperature range 1–20 K, depending on the electron density and the device quality. In this temperature range $kT\tau_e/\hbar$ is in the range 0.1–1.6, where τ_e is of order 6×10^{-13} s for our devices. When T is below 1 K, $1/\tau_i$ is linearly dependent upon temperature.[8,9]

Owing to the small Fermi energy associated with silicon inversion layers as compared with that of metals, the

electron-electron scattering rate is greatly enhanced. In fact, in silicon inversion layers, the electron-electron scattering rate is believed to be larger than the phonon scattering rate below 4.2 K (Ref. 10); this provides us with the opportunity of observing electron-electron scattering directly from the conductivity measurement. In metals this interaction is often obscured by the phonon scattering.[11,12] But unlike some metals in which the Fermi surfaces are anisotropic or extend beyond half of the Brillouin zone, the momentum-conserving part of the interaction in silicon (100) inversion layers cannot contribute to the resistivity. The reason for this is that for the usual range of electron density, the Fermi surface is isotropic with a very small Fermi wave vector (less than 5×10^8 m^{-1}) compared to the reciprocal-lattice vector. Thus the total velocity vector is conserved and umklapp processes are not allowed. In this case, only the scattering rate given in Eq. (3) is able to relax an electron current in the silicon (100) case. For silicon (100) inversion layers, it is known that the temperature-dependent part of the scattering deduced from the resistivity measurement is linearly proportional to T below 4.2 K and depends on the impurity concentration[10] and hence is consistent with the argument. There has been an alternative explanation to the linear temperature dependence of the resistivity. The change of resistivity may be due to the temperature dependence of the screening effect on the electron-impurity potential. Therefore, in order to study this issue in greater detail, in this paper we try to see if the inelastic scattering rate deduced from the magnetoconductance measurement is indeed separable into two parts which are consistent with Eqs. (2) and (3), in the $kT\tau_e/\hbar\sim1$ region. The momentum-nonconserving part of the inelastic scattering can then be compared with the resistivity data.[10] An attempt to separate $1/\tau_i$ into two parts can also be found in the work by Uren *et al.*[5] for a single electron density.

III. EXPERIMENTAL CONSIDERATION AND RESULT

The object of the present work is to try to verify the inelastic scattering rate expressions given in the preceding section. In this way, more evidence can be provided for the theoretical calculation of the electron-electron scattering rate, and hence confirm whether this interaction is indeed the relevant process to delocalize the electrons.

At the outset, some preliminary remarks on the parameters of the experimental samples should be made. The first one is the quality of the samples. Intuitively, one may think that the localization effect is stronger when the system is more disordered. The effect should then be more easily observable in lower quality devices. However, this is only true in the strong-localization region. In the weak-localization region where perturbation theory can be applied, the correction to the conductivity is in fact approximately independent of the device quality. This is because such a correction is also dependent on the lifetime of the electrons. The longer the lifetime, the larger is the correction. However, in the disordered system, the lifetime gets shorter as the concentration of the impurity increases. It turns out that the correction is approximately the same for devices with different impurity concentration, but increases with the electron density N_s.

When a magnetic field is applied, the critical field (H_c), above which the localization effect is quenched, turns out to be very sensitive to the disorder of the material. Here, we provide some estimate of this field.

In the localization theory, the change of dc conductivity at $H=0$ is given by[13]

$$\frac{\delta\sigma}{\sigma}=-2\tau_e^2\int\frac{d^2q}{(2\pi)^2}\frac{1}{2\pi N_1\tau_e^2\hbar}\frac{1}{Dq^2+1/\tau_i}\ . \tag{4}$$

The limit of integration is from $q_{\min}=0$ to $q_{\max}=(D\tau_e)^{1/2}$. However, in a magnetic field, the electron-pair states condense into Landau levels,

$$\frac{\delta\sigma}{\sigma}=-2\tau_e^2\sum_{n=0}^{n_m}\frac{\mathscr{D}(n)}{2\pi N_1\tau_e^2\hbar[(4DeH/\hbar)(n+\frac{1}{2})+1/\tau_i]}\ , \tag{5}$$

where $\mathscr{D}(n)$ is the number of states in the level n. Increasing the magnetic field causes Landau levels to move away from the origin in q space. As the divergence of $\delta\sigma$ comes from the states near the origin, the effect of the magnetic field is to reduce the effect of localization. When the first Landau level is beyond $q_{\max}$, most of the localization should have been canceled out. The critical field (H_c) corresponds to the radius of the first Landau level in the q space equal to $q_{\max}$. Hence from Eq. (5), $2eH_c/\hbar=1/D\tau_e$ or $H_c=\hbar/el_e^2$. Here, $l_e=v_F\tau_e$ is the elastic scattering length. For a sample with mobility $\mu=2000$ $cm^2/V\,s$, $l_e=2.5\times10^{-8}$ m, H_c corresponds to 5.4 kG. But for samples with $\mu=10\,000$ $cm^2/V\,s$, $l_e=1.2\times10^{-7}$ m, H_c can be as low as 200 G. Hence, while working with high-mobility samples, one can apply a much weaker magnetic field to get the desired signal. In this way, one can avoid the complication arising from another quantum effect, namely the electron-electron interaction. This is important in extracting the parameter τ_i.

In a disordered system, besides the effect of localization, there is another quantum correction in the conductivity due to the electron-electron interaction. The electron-electron interaction reduces the density of states at the Fermi level and hence decreases the conductivity. At zero magnetic field $\delta\sigma$ is given by[14]

$$\delta\sigma=-\frac{e^2}{\hbar}\frac{1}{2\pi^2}(g_1+g_2-2g_3-2g_4)\ln\frac{\hbar}{4\pi\tau_e kT}\ , \tag{6}$$

where $g_1=1$ and $2g_3=F\sim0.8$ in Ref. 5.

When magnetic field is applied, only g_2 and g_4 processes give strong orbital magnetic effect. The change of conductivity $\Delta\sigma(H)$ at constant temperature is given by[14]

$$\Delta\sigma(H,T_{\text{const}})=\frac{e^2}{\hbar}\frac{1}{2\pi^2}(g_2-2g_4)\phi(h,\gamma)\ , \tag{7}$$

where

$$\gamma=\frac{\hbar}{2\pi\tau_i kT}\ ,$$

$$h=\frac{2De\tau_e H}{\hbar}\ ,$$

$$\phi(h,\gamma)=-\sum_{l=1}^{\infty}\left\{5\left[\frac{l}{(\gamma h)^2}\Psi''\left[\frac{1}{2}+\frac{1}{h}+\frac{l}{\gamma h}\right]+\frac{l}{(l+\gamma)^2}\right]+6\left[\frac{l}{2(\gamma h)^3}(l+\gamma)\Psi'''\left[\frac{1}{2}+\frac{1}{h}+\frac{l}{\gamma h}\right]-\frac{l}{(l+\gamma)^2}\right]\right\},$$

and $\Psi^{(n)}$ is the polygamma function.

The functional dependence of $\phi(h,\gamma)$ is very different from that obtained in the localization theory. If the magnitudes of the two effects are comparable in size, one will not be able to separate out the individual contributions and extract τ_i. Fortunately, when one works with high-mobility samples, the variables γ and h are small, hence $\phi(h,\gamma)$ is small. For example, for our device parameter, $\tau_i=4\times10^{-11}$ s and $H=100$ G, we obtain $\gamma=0.03/T$ and $h=20$. When $T>1$ K, the contribution of the interaction effect to the magnetoconductance is only 4% of that due to localization effect. Here, we have assumed the coupling constants $g_2\sim g_4\sim F/4$ suggested by Fukuyama.[16] It is pointed out by Lee and Ramakrishnan[17] that the coupling constants g_2 and g_4 should be replaced by an effective coupling

$$g_i=\frac{g_i}{1+g_i\ln(E_F/kT_0)} \tag{8}$$

where $i=2,4$ and $T_0=\max(T,DeH/k)$.

So, the contribution is reduced further by a factor of 2. One notices that if a magnetic field of 5.4 kG is applied, the interaction effect will not be negligible.

In addition to the orbital effect, there is also a magnetoresistance effect due to the addition of the Hartree interaction of up- and down-spin electrons.[17] It is much smaller than the magnetoconductance effect due to localization by a factor of 10^{-4} at fields below 100 G. Hence, we can attribute all the effect at low field to the effect of localization. In the following experiment, the maximum mobilities of the devices used at 4.2 K is between 13 000 and 18 000 $\mathrm{cm^2/V\,s}$. For magnetic fields up to 100 G, localization theory can be safely applied. Also, in this work τ_i is assumed to be independent of small magnetic fields.

Magnetoconductance measurements have been done on silicon inversion layers in (100) orientation for three samples between 1 and 4.2 K. In this temperature range, we expect the two electron-electron scattering rates given by Eqs. (2) and (3) to be comparable. The maximum applied magnetic field is 100 G. The experimental procedure and the way to extract τ_i are based on previous work.[7] The devices used are of long bar structure, so that we are actually measuring ρ_{xx} instead of σ_{xx}. When $T<4.2$ K the electrons are highly degenerate, σ_{xx} can be assumed to be $1/\rho_{xx}$ with error in determining $\Delta\sigma$ much less than 1% at magnetic fields up to 100 G. A satisfactory fit to the experimental curves are obtained by varying a single parameter (τ_i) in the following expression with $N_v\alpha=1$ (Ref. 16):

$$\Delta\sigma(H,T_{\text{const}})=\frac{e^2}{\hbar}\frac{N_v\alpha}{2\pi^2}\left[\psi\left[\frac{1}{2}+\frac{\hbar}{4DeH\tau_i}\right]-\psi\left[\frac{1}{2}+\frac{\hbar}{4DeH\tau_e}\right]+\ln\frac{\tau_i}{\tau_e}\right], \tag{9}$$

where ψ is the digamma function.

Since data from the three devices are qualitatively the same, we will only present data from device ABT105. In analyzing the data, since the range of the temperature is small, the factor $\ln(E_F/kT)$ in Eq. (2) varies within the range 4.7 ± 0.7, which is much less sensitive than the T^2 factor in the front. So, we treat the factor $\ln(E_F/kT)$ as a function of E_F. Including the E_F dependence in the prefactor, we make a further simplification by assuming τ_i from Eq. (2) proportional to E_F^{λ} for some constant λ. We expect λ is approximately equal to 1. Since E_F is directly proportional to N_s in 2D, τ_i is expected to be proportional to N_s^{λ} in the ordered regime. For Eq. (3), since the constant T_1 is a constant of order 4.6×10^{10} K for $D=87$ $\mathrm{cm^2/s}$ and $\kappa=1.45\times10^8$ $\mathrm{cm^{-1}}$, $\ln T/T_1$ is effectively a constant of order 25. Here, κ is equal to $2\pi Ne^2$. Using Matthiessen's rule, we express the total $1/\tau_i$ as[5]

$$\frac{1}{\tau_i}=\frac{A'}{N_s^{\lambda}}T^2+\frac{B'}{N_s\tau_e}T\ , \tag{10}$$

where A' and B' are independent of N_s, τ_e, and T.

The first term of this expression is for the momentum-conserving part and the second term is for the nonconserving part of the electron-electron interaction. We can also express Eq. (10) as

$$\frac{1}{\tau_i}=AT^2+BT\ , \tag{11}$$

where A and B are coefficients independent of T and are functions of N_s and τ_e only.

In order to extract coefficients A and B as a function of electron density, magnetoconductance effect is measured at a fixed value of electron density at different temperatures. The values of τ_i at different temperatures can be deduced from the magnetoconductance expression Eq. (9). Since at fixed N_s, A and B are constants, we can fit the experimentally determined $1/\tau_i$ as a function of T to the form of Eq. (11) and obtain the values of A and B. This procedure is repeated for different electron densities, and hence we can obtain the values of A and B at different electron densities. The result of the N_s dependence of A and the $N_s\tau_e$ dependence of B can be compared with Eq. (10). Figure 1 shows some typical τ_i-vs-$1/T$ plots for different electron densities for device ABT105. The range of electron density is from 0.8×10^{16} $\mathrm{m^{-2}}$ to 4.8×10^{16} $\mathrm{m^{-2}}$. If $1/\tau_i$ is depicted a combination of power laws, then curves in Fig. 1 should not be straight lines. However, from the plot, since the data show only slight deviation from the straight lines in this temperature range, we can characterize τ_i by a single power law. So if we write

$$\tau_i=C\left[\frac{1}{T}\right]^p\ , \tag{12}$$

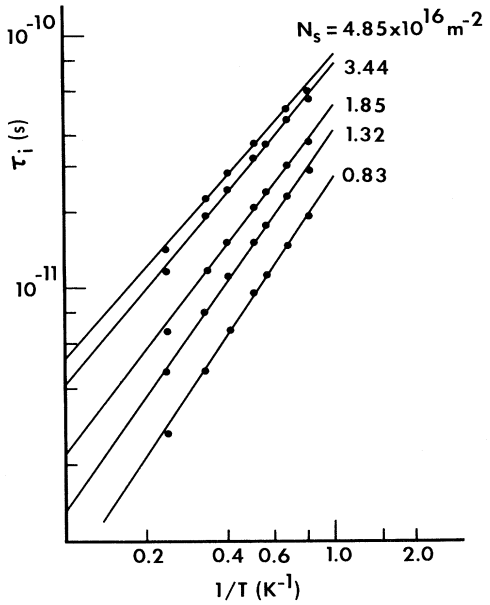

FIG. 1. Graph of τ_i vs $1/T$ in the log-log scale for different N_s. The data are almost linear and the slope decreases as N_s increases ($V_{sub} = -1.5$ V).

where C and p are constants, then we can extract the power p from the slope of the curves. Again, the power p is plotted against N_s in Fig. 2. The range of p lies between 1 and 2 as expected. In the same graph, we also plot τ_e vs N_s, where τ_e is based on conductivity measurement at 4.2 K. The curves show there is a strong correlation between τ_e and p. This can be understood if we assume Eq. (10). When τ_e gets smaller as N_s increases, the linear term is more dominant. Hence, p gets closer to 1 as the experimental results in Fig. 2 shows.

In order to extract the coefficient A and B from the data, A and B are chosen such that τ_i from Eq. (11) coincides with that obtained by Eq. (12) from 1 to 4 K. We can verify this gives a good estimation of A and B by replotting the curves based on A and B chosen along with the experimental data. Figure 3 shows two typical plots.

Next, to verify the second term of Eq. (10), we plot $B\tau_e$ vs $1/N_s$ in Fig. 4 with two different substrate biases. The

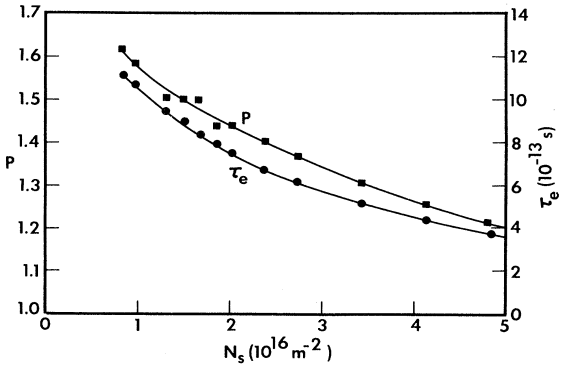

FIG. 2. Graph of p and τ_e vs N_s for $V_{sub} = -1.5$ V. p and τ_e show a strong correlation.

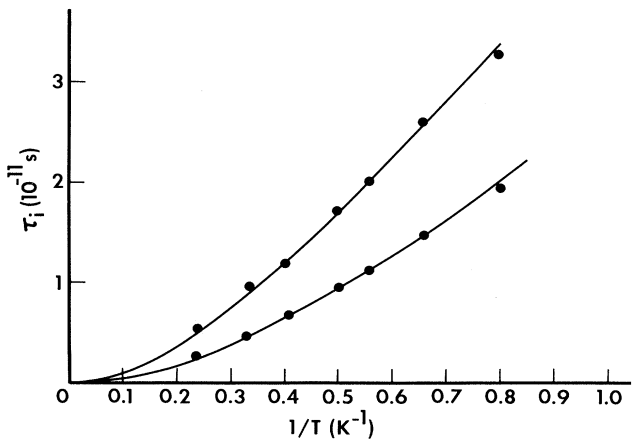

FIG. 3. Graph of τ_i vs $1/T$ for $N_s = 0.850\times10^{16}$ and 1.495×10^{16} m^{-2}. The dotted points are experimental data. The curves are based on A and B chosen.

substrate bias can change τ_e slightly for a fixed N_s. For substrate bias voltage $V_{sub} = -1.5$ V, we obtain from the curves $B = 1.65\times10^{14}/N_s\tau_e$, and for $V_{sub} = -9$ V, $B = 1.525\times10^{14}/N_s\tau_e$. The curves show that the functional dependence of B on $N_s\tau_e$ agrees with the inelastic scattering in the diffusive region. However, the magnitude is smaller than the prediction from Eq. (3). Namely, at $N_s = 2\times10^{16}$ m^{-2}, τ_e is 7.4×10^{-13} s with D equal to 8.7×10^{-3} m^2/s; the experimental value is $1/\tau_i = 1.1\times10^{10}T$ s^{-1} in comparison with the theoretical value $1.2\times10^{11}T$ s^{-1}. This discrepancy has been explained by arguing that the strength of the Coulomb interaction in silicon substrate should be weakened due to the dielectric polarization[8] of the material. However, if the dielectric property is considered, the inverse screening length is also reduced by the same factor, so that in the

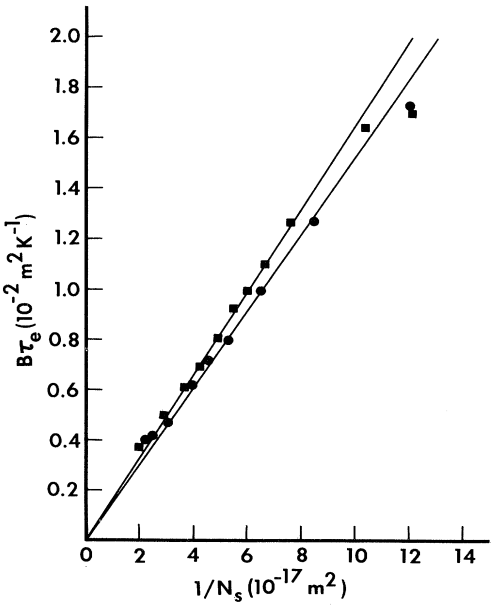

FIG. 4. Graph of $B\tau_e$ vs $1/N_s$, with the square points for $V_{sub} = -1.5$V and the dotted points for $V_{sub} = -9$ V.

small-q approximation the scattering rate is in fact independent of the dielectric constant of silicon. This case also applies to the scattering rate in the ordered limit. So, in fact, the discrepancy arises from the approximation taken in Eq. (3) since it only applies to the case in which the frequency of the external excitation (ω) is much less than $kT/\hbar$. However, for a system in thermal equilibrium without external excitation, the electron-density fluctuation is due to the thermal excitation, which has the characteristic frequency $kT/\hbar$. So, the above criterion is not met and the theoretical magnitude should be reduced. This can be seen in the other limit of the formalism that when T approaches zero with ω finite, the scattering rate is given by Eq. (3) without the logarithmic term[3] and the rate is greatly reduced.

In Fig. 5, the value of A is plotted against $1/N_s$ for $V_{\text{sub}}=-1.5$ V and $V_{\text{sub}}=-9$ V, respectively. We obtained from the curves $A=7.405\times10^{30}/N_s^{1.293}$ for $V_{\text{sub}}=-1.5$ V and $A=9.045\times10^{30}/N_s^{1.185}$ for $V_{\text{sub}}=-9$ V. The magnitude of this term is in good agreement with the prediction given by Eq. (2). For instance, the experimental value at $N_s=2\times10^{16}$ m^{-2} is $1/\tau_i=5.9\times10^9T^2$ s^{-1}, as compared with that given by Eq. (2), $1/\tau_i=6.1\times10^9T^2$ s^{-1}. On the other hand, the experimental dependence of $1/\tau_i$ on N_s is slightly higher than the prediction. This may be due to the fact that in the formalism, the interaction potential is approximated by using the small-q and -ω limits. Nevertheless, on the whole, we find good agreement between theory and experiment with the estimated experimental error around 10%.

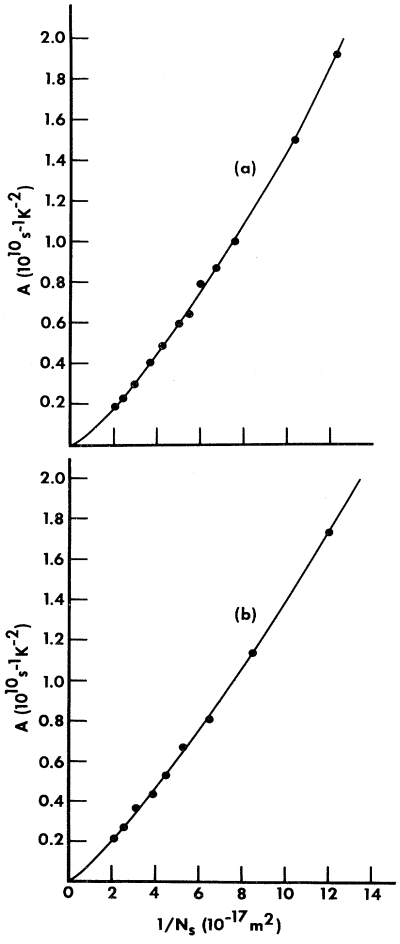

FIG. 5. Graph of A vs $1/N_s$ for (a) $V_{\text{sub}}=-1.5$ V, and (b) $V_{\text{sub}}=-9$ V.

In addition to the above result, for another device of similar quality, we also find at $V_{\text{sub}}=0$ V,

$$\frac{1}{\tau_i}=1.5\times10^{31}\frac{T^2}{N_s^{1.3}}+2.3\times10^{14}\frac{T}{N_s\tau_e},$$

which shows the consistency of the experimental result.

IV. FURTHER DISCUSSION

Summing up the result from the last section for ABT105 at $V_{\text{sub}}=-1.5$ V, we get

$$\frac{1}{\tau_i}=7.41\times10^{30}\frac{T^2}{N_s^{1.298}}+1.65\times10^{14}\frac{T}{N_s\tau_e} \tag{13}$$

(in units of s^{-1}). As mentioned before, the second term does not conserve total momentum of the electron gas. Thus we expect this term to affect an electric current. With this in mind we can write, from Eq. (10), the resistivity (ρ), before the localization effect is important, as

$$\rho=\frac{m^*}{N_se^2}\left[\frac{1}{\tau_e}+\frac{1}{\tau_T}\right], \tag{14}$$

$$\frac{1}{\tau_T}=\beta\frac{T}{N_s\tau_e}, \tag{15}$$

(the latter in units of s^{-1}), where β is a constant with the same magnitude as B'. Here, the first term is from the elastic electron-impurity scattering. The second term is from the inelastic scattering event between electrons without conserving momentum. Hence, the resistivity has an explicit linear temperature dependence, even assuming the electron-impurity interaction is independent of temperature. The temperature dependence is weak because the typical experimental value of $1/\tau_i$ is only 3% of $1/\tau_e$.

Before, there were theoretical works on the temperature dependence of $1/\tau_e$. $1/\tau_e$ is found to have negligible temperature dependence by using the $q\rightarrow0$ approximation[18] on the static screening or a linear dependence by using q-dependent screening.[19] However, in the q-dependent formalism, the temperature-dependent part has a $(N_s\tau_e)^{-2}$ dependence for Coulomb scattering and a $N_s^{1.3}$ dependence for surface roughness scattering instead of a $(N_s\tau_e)^{-1}$ dependence proposed above. Therefore, the N_s and τ_e dependences may distinguish the two models. Here, we find the experimental report from Cham and Wheeler[10] is suitable for our discussion.

If we follow Eq. (14) and assume τ_e is temperature independent, we get $(\delta\rho/\rho)/\delta T=\beta/N_s$. Here, the condition that $1/\tau_T\ll1/\tau_e$ has been used. So the quantity $(\delta\rho/\rho)/\delta T$ should be independent on the device quality for fixed N_s. In Fig. 6, the variation of ρ with T is shown for two devices of very different quality by a factor of 5. The quantity $(\delta\rho/\rho)/\delta T$ can be extracted in the linear region. For $\delta T=1$, $\delta\rho/\rho=0.017$ for device A1(80) and

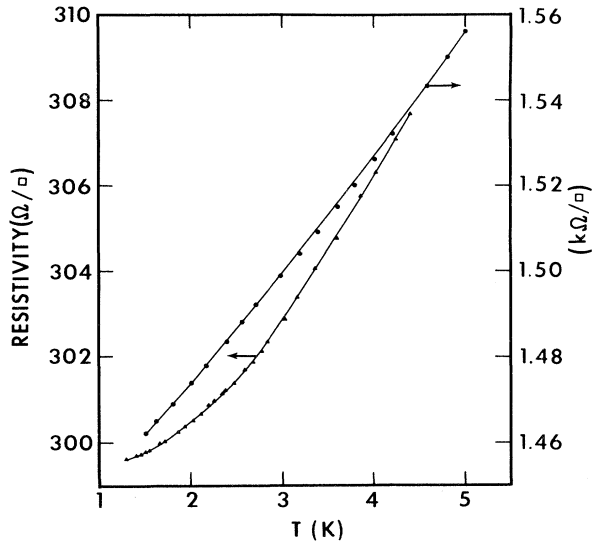

FIG. 6. Resistivity vs T. ●: Al (80), $N_s=1.2\times10^{12}$ cm^{-2}, $V_{sub}=-9.4$ V. ▲: R3L, $N_s=1.3\times10^{12}$ cm^{-2}, $V_{sub}=-17.3$ V.

$\delta\rho/\rho=0.011$ for device R3L. The result is indeed almost independent of the device quality. If we use $\beta=B'$ from ABT105, we get $\delta\rho/\rho=0.014$ for the former, and $\delta\rho/\rho=0.013$ for the latter, which is in good agreement with the experimental result. One notices that if other τ_e dependence for the temperature-dependent term of ρ had been used, the quantity $(\delta\rho/\rho)/\delta T$ would be dependent upon the device quality.

Further evidence is provided in Fig. 7. This figure shows the relationship of $1/\tau_T$ and the maximum mobility (μ_m) at fixed $N_s=1.5\times10^{16}$ m^{-2} and at $T=4.5$ K for 10 different devices. $1/\tau_T$ is deduced from the temperature-dependent part of the resistivity measurement. If we assume Eq. (15), for fixed N_s, $1/\tau_T$ should be proportional to $1/\tau_e$, which in turn is proportional to $1/\mu$. For most devices in the figure, the mobility (μ) as a function of N_s has a plateau region around $N_s=1.5\times10^{16}$ m^{-2}. So that, at this N_s, $1/\mu$ is approximately equal to $1/\mu_m$. So, we expect $1/\tau_T$ to be approximately proportional to $1/\mu_m$. From the figure, we obtain the slope of the best straight line to be -1. So we can again deduce that $1/\tau_T$ is linearly proportional to $1/\tau_e$. Furthermore, the data is consistent with the value of τ_T given by $1/\tau_T=10^{14}T/N_s\tau_e$, universal to the silicon inversion layers.

Now, we turn to examine the relationship between $1/\tau_T$ and N_s. Since τ_e is usually a function of N_s, we cannot keep τ_e constant and vary N_s conveniently; so the comparison is not as simple. In Fig. 8, the experimental $1/\tau_T$ data of two devices A13 and TA15 are plotted and are labeled as (1) and (3), respectively. Again, we compute $1/\tau_T$ based on Eq. (15) with $\beta=1.65\times10^{14}$ and obtain curves (2) and (4) for A13 and TA15, respectively. Both are in good agreement with the experiment.

Therefore, indeed, from the experimental results, τ_T is given by $1/\tau_T=\beta T/N_s\tau_e$ with β of order 10^{14} for silicon inversion layers. The above data does not support the q-dependent screening theory. One explanation is that, when the temperature is less than 4 K, the parameter $kT\tau_e/\hbar$ is less than 0.5 for all N_s larger than 1×10^{16} m^{-2}. The smearing of the Fermi surface in this temperature range is hence mainly due to disorder rather than temperature. As the q-dependent screening theory depends on the increase of the thermal spreading of the Fermi surface with the temperature, the effect is small for usual devices at low temperature.

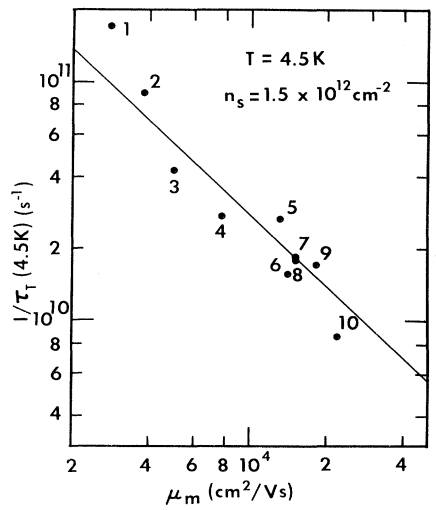

FIG. 7. $1/\tau_T$ at 4.5 K and $N_s=1.5\times10^{12}$ cm^{-2}. Our data have been interpolated to a fixed N_s and T whenever necessary to simplify discussions. Device label and V_{sub} (V) are (1) TA15, -9.41; (2) Al(80), -9.42; (3) M72-31H, -6.27; (4) M72-31, -6.27; (5) Al3, -6.29; (6) M72-14, -1.25; (7) Thl, -9.41; (8) R3L, -9.42; (9) B15, 0; (10) A(2500), -9.41.

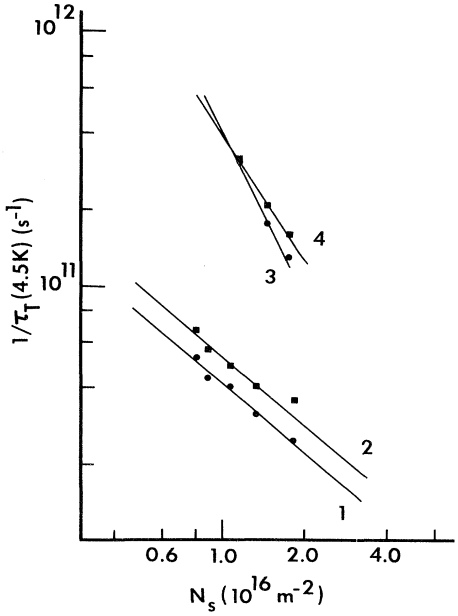

FIG. 8. (1) A13 data; (2) with the use of the equation $1/\tau_T=1.65\times10^{14}T/N_s\tau_e$; (3) TA15 data; (4) with the use of equation $1/\tau_T=1.65\times10^{14}T/N_s\tau_e$.

V. CONCLUSION

In this work, we have shown that the result of the diffusive limit alone is not adequate in describing a system in the $kT\tau_e/\hbar \sim 1$ regime, but must be implemented by the momentum-conserving part. The experimental result shows the measured inelastic scattering rate separable into a T^2 term and a T term which agree with the theoretical prediction in both limits. In this way, we have given more evidence to support the idea that the electron-electron interaction is indeed the physical mechanism to delocalize an electron.

As the inelastic scattering formulated in the diffusive regime does not conserve total momentum, it is able to affect an electric current. The part of $1/\tau_i$ that depends linearly on T deduced from the magnetoconductance measurements is in good agreement with $1/\tau_T$ obtained from the temperature variation of resistivity and hence consistent with the idea.

But in order to confirm the above model, more experimental and theoretical work is needed. In the formalism of the electron-electron interaction in the diffusive regime, the impurities are certainly involved in the mutual interaction among the electrons, although the role is not very apparent. The missing momentum during the interaction of the electrons must be transfered to the impurities. In order to have a better understanding of the electron-electron interaction in this regime, the exact role of the impurities in the electron-electron interaction deserves a further investigation. This poses an interesting theoretical problem in this subject.

Experimentally, it is interesting to note that if the surface of the silicon substrate is other than (100) surface, the momentum-conserving part of the electron-electron interaction should also contribute to the resistivity. This is because the velocity vector is not conserved due to the different effective mass in different directions. In this case, the temperature dependence of the resistivity at low temperature should deviate from the linear relationship.

Another possible way of testing the model is to investigate the temperature dependence of the resistivity of very narrow channels. In this case, the momentum-nonconserving electron-electron interaction is proportional to $T^{1/2}$ instead of T. At present, the author is not aware of any definite experimental result showing such variation.

Note added. While revising this paper, the author noticed a similar analysis of τ_i done by Davies and Pepper.[20] Although some of the interpretations of the results are not the same, the experimental data agrees with the result of this work. For example, at $N_s \sim 2\times 10^{16}$ m^{-2}, they found $1/\tau_i = 5.1\times 10^9 T^2 + 3.0\times 10^{10} T$ s^{-1} for $k_F l = 11$. Here, we found $1/\tau_i = 5.9\times 10^9 T^2 + 1.1\times 10^{10} T$ s^{-1} for $k_F l = 28$. The fact that $N_v\alpha = 0.76$ in their analysis for higher magnetic field and lower mobility samples is consistent with the argument given in this work. The interaction effect is significant in their case.

ACKNOWLEDGMENT

I would like to thank Professor R. G. Wheeler for very fruitful discussions. Supported in part by the National Science Foundation through Grant No. DMR-8213080.

[1]A. Schmid, Z. Phys. 271, 251 (1974).
[2]G. F. Giuliani and J. J. Quinn, Phys. Rev. B 26, 4421 (1982).
[3]E. Abrahams, P. W. Anderson, P. A. Lee, and T. V. Ramakrishnan, Phys. Rev. B 24, 6783 (1981).
[4]H. Fukuyama and E. Abrahams, Phys. Rev. B 27, 5976 (1983).
[5]M. J. Uren, R. A. Davis, M. Kaveh, and M. Pepper, J. Phys. C 14, 5737 (1981).
[6]Y. Kawaguchi and S. Kawaji, Surf. Sci. 113, 505 (1982).
[7]R. G. Wheeler, Phys. Rev. B 24, 4645 (1982).
[8]D. J. Bishop, R. C. Dynes, and D. C. Tsui, Phys. Rev. B 26, 773 (1982).
[9]R. G. Wheeler, K. K. Choi, A. Goel, R. Wisnieff, and D. E. Prober, Phys. Rev. Lett. 49, 1674 (1982).
[10]K. M. Cham and R. G. Wheeler, Phys. Rev. Lett. 44, 1472 (1980).
[11]W. E. Lawrence and J. W. Wilkins, Phys. Rev. B 7, 2317 (1973).
[12]H. van Kempen, J. H. J. M. Ribot, and P. Wyder, J. Phys. F 11, 597 (1981).
[13]B. L. Altshuler, D. Khmel'nitzkii, A. I. Larkin, and P. A. Lee, Phys. Rev. B 22, 5142 (1980).
[14]H. Fukuyama, J. Phys. Soc. Jpn. 50, 3407 (1981).
[15]B. L. Altshuler, A. G. Aronov, and P. A. Lee, Phys. Rev. Lett. 44, 1288 (1980).
[16]H. Fukuyama, Surf. Sci. 113, 489 (1982).
[17]P. A. Lee and T. V. Ramakrishnan, Phys. Rev. B 26, 4009 (1982).
[18]F. Stern and Howard, Phys. Rev. 163, 816 (1967).
[19]F. Stern, Phys. Rev. Lett. 44, 1472 (1980).
[20]R. A. Davies and M. Pepper, J. Phys. C 16, L353 (1983).